Numerical tools to study hydrogen flame acceleration

WCCM ECCOMAS Congress 2021

January 11-15, 2021

Luc Lecointre

Sergey Kudriakov[1], Etienne Studer[1], Ronan Vicquelin[2], Christian Tenaud[3]

[1] Université Paris Saclay, CEA, Service de Thermo-hydraulique et de mécanique des fluides, 91191, Gif sur Yvette, France

[2] Université Paris Saclay, CNRS, CentraleSupélec, Laboratoire EM2C, 91190, Gif-sur-Yvette, France

[3] Université Paris Saclay, CNRS, LIMSI, 91400, Orsay, France

Introduction

Introduction

Inflammable gas dynamics in confined environment

- Storage of flammable gas
- Release of hydrogen in core reactor during nuclear accident

Dynamic behaviour of the flame

- Flame acceleration
- Transition to Detonation
- Influence of concentration gradients [1], geometrical configuration...

Experimental Setup [2]

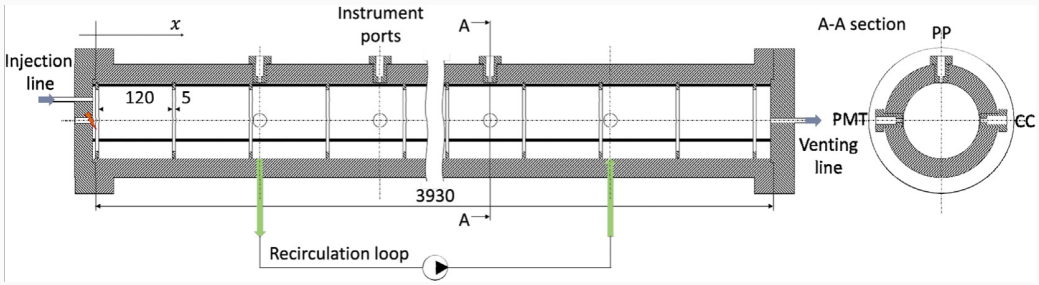

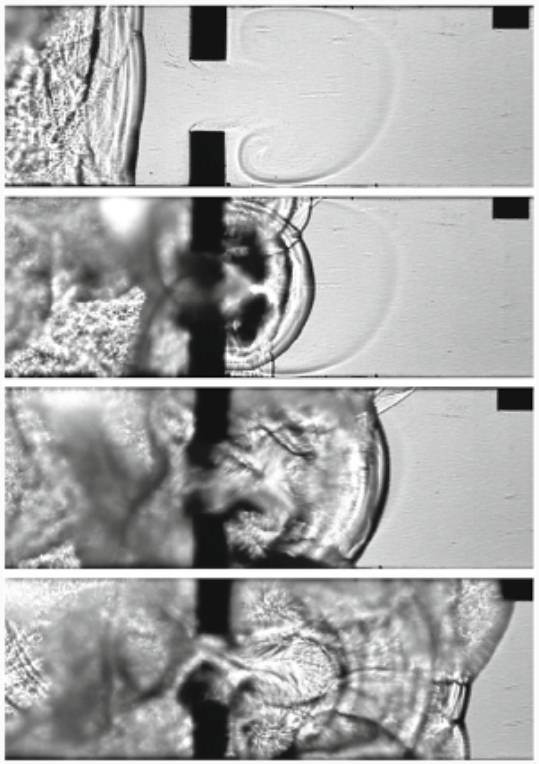

Figure 1 – Shadowgraph sequence of DDT inside obstacle with vertical concentration gradient[1]

1. Boeck et al., *Shock Waves* (2016).
2. Scarpa et al., *International Journal of Hydrogen Energy* (2019).

Flame acceleration and transition to detonation

Flame acceleration phenomena

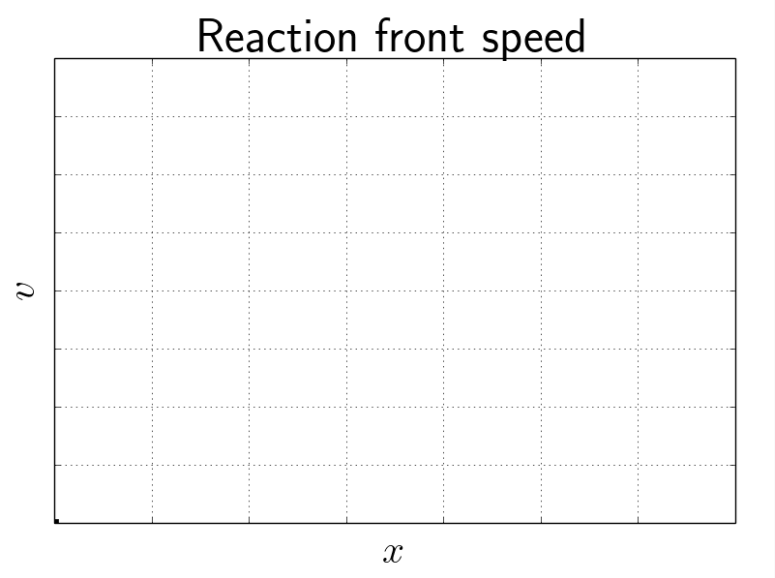

Flame acceleration and transition to detonation

Flame acceleration phenomena

- Thermodiffusive instabilities ($Le < 1$ flame wrinkling)

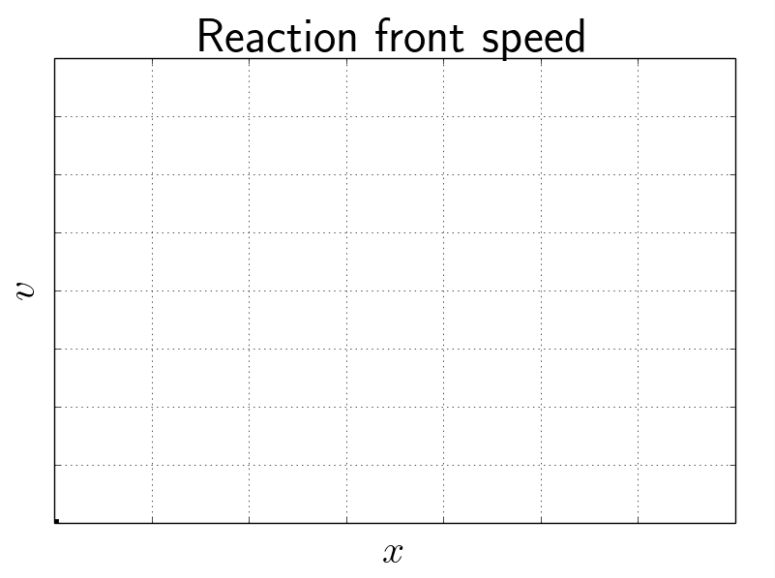

Flame acceleration and transition to detonation

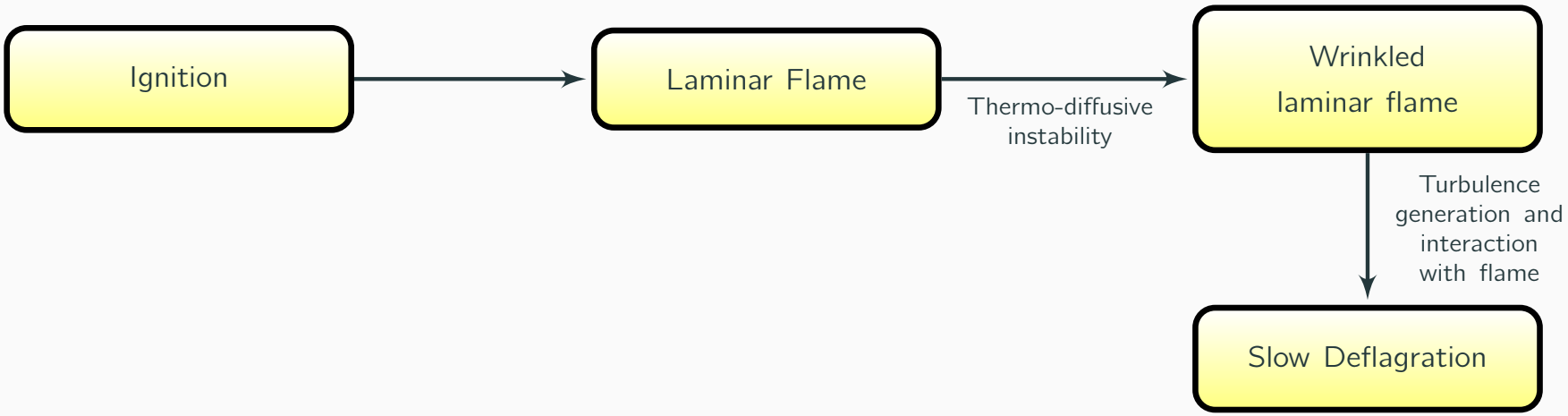

Flame acceleration phenomena

- Thermodiffusive instabilities ($Le < 1$ flame wrinkling)
- Turbulence generation

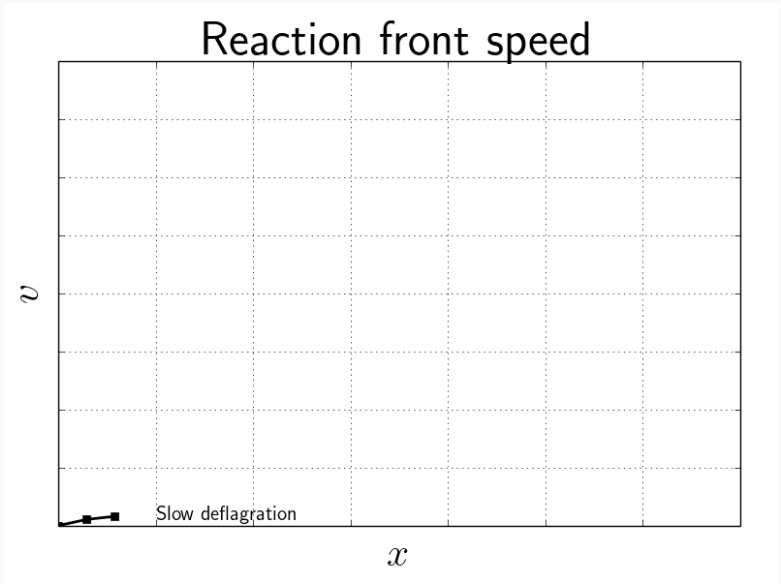

Flame acceleration and transition to detonation

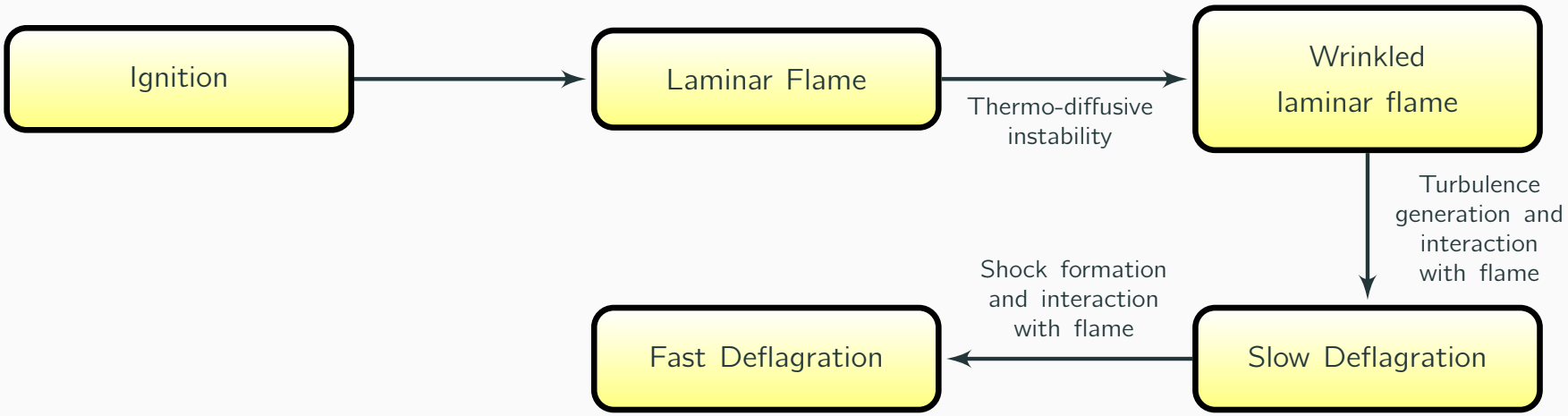

Flame acceleration phenomena

- Thermodiffusive instabilities ($Le < 1$ flame wrinkling)
- Turbulence generation
- Shock interaction : Richtmyer Meshkov instability

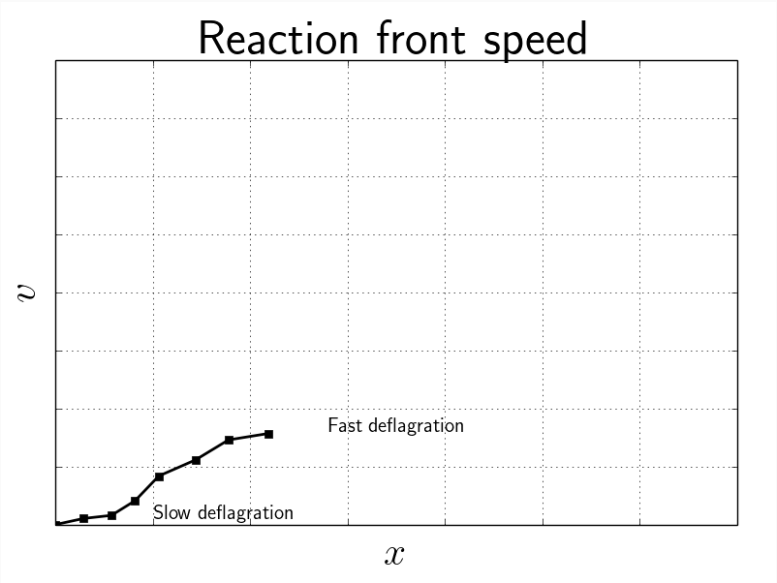

Flame acceleration and transition to detonation

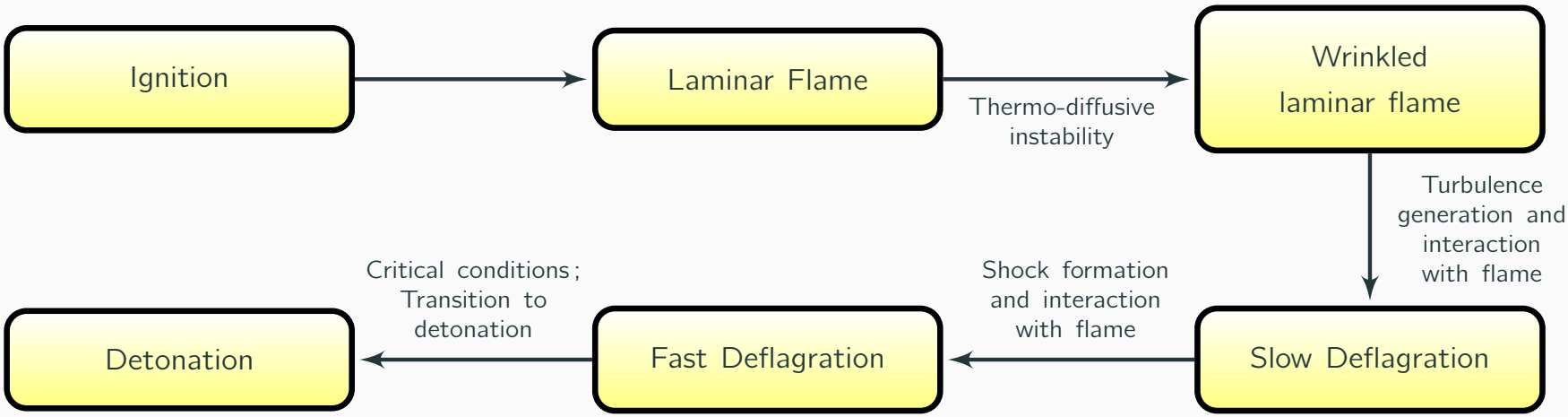

Flame acceleration phenomena

- Thermodiffusive instabilities ($Le < 1$ flame wrinkling)
- Turbulence generation
- Shock interaction : Richtmyer Meshkov instability

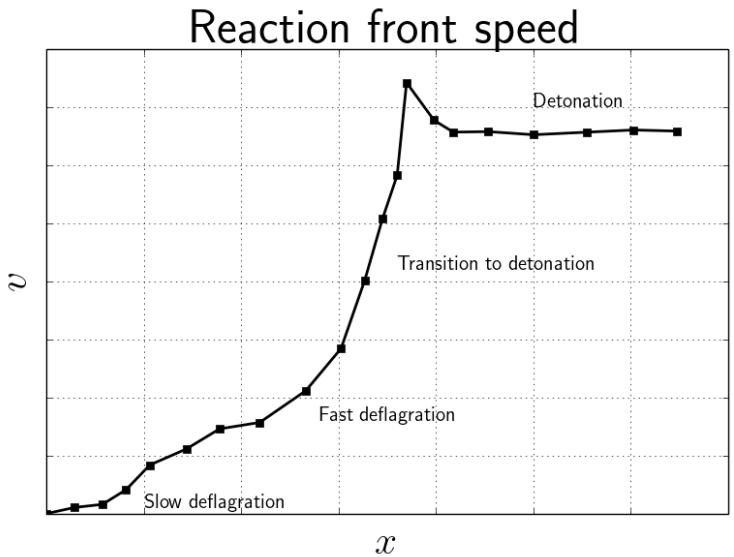

Flame acceleration and transition to detonation

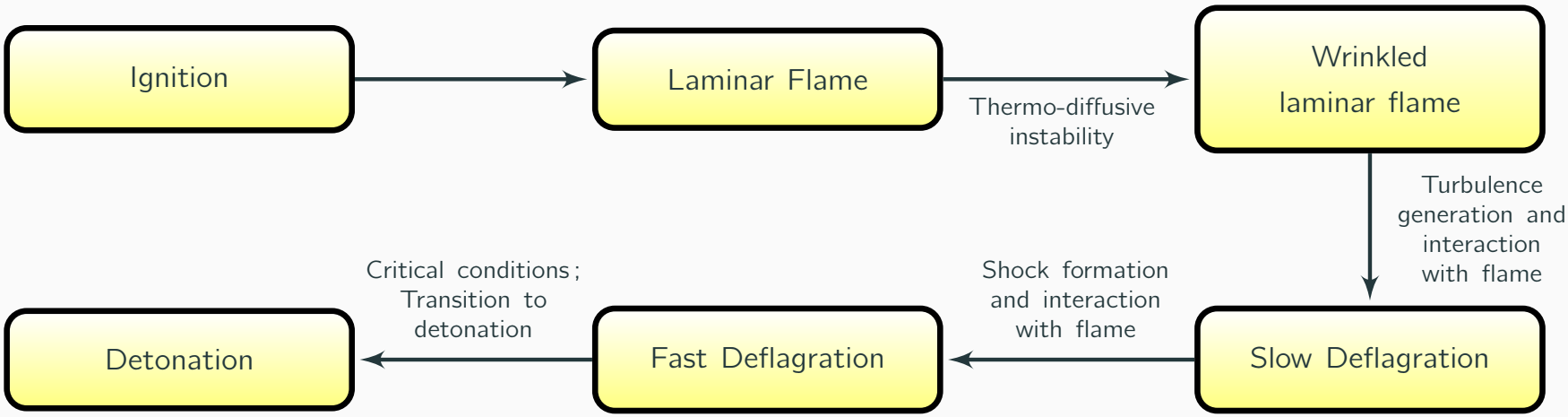

Flame acceleration phenomena

- Thermodiffusive instabilities ($Le < 1$ flame wrinkling)
- Turbulence generation
- Shock interaction : Richtmyer Meshkov instability
- Impact of geometrical configuration : turbulent vortex, local hot spots...

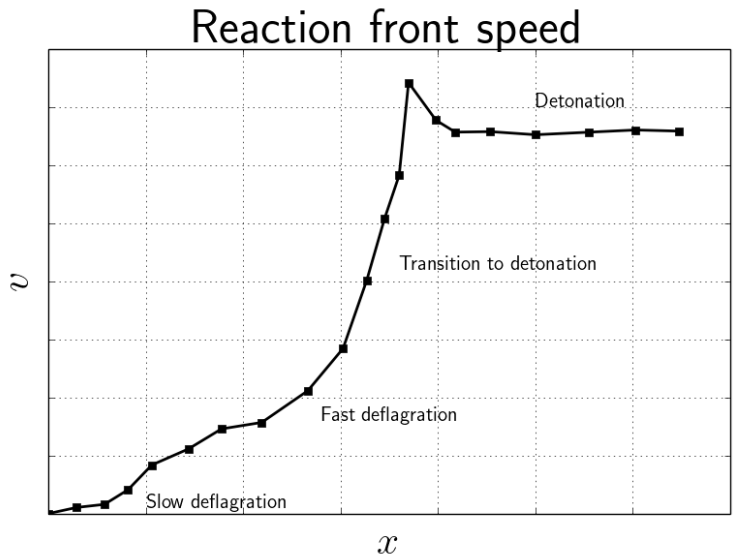

Numerical tools/MR_CHORUS solver

Navier-Stokes equation

$$\mathbf{w}_t + \nabla \cdot (\mathbf{F}^E(\mathbf{w}) - \mathbf{F}^V(\mathbf{w}, \nabla \mathbf{w})) = \mathbf{S}(\mathbf{w}), \quad \text{with} \quad \mathbf{w} = (\rho Y_1, ..., \rho Y_{ns}, \rho \mathbf{u}, \rho E)^T \tag{1}$$

Numerical challenges [3]

- Multiscales in time and space
- Compressible effects
- Non callorically perfect gas

3. Tenaud, Roussel et Bentaleb, *Computers & Fluids* (2015).

Numerical tools/MR_CHORUS solver

Navier-Stokes equation

$$\mathbf{w}_t + \nabla \cdot (\mathbf{F}^E(\mathbf{w}) - \mathbf{F}^V(\mathbf{w}, \nabla \mathbf{w})) = \mathbf{S}(\mathbf{w}), \quad \text{with} \quad \mathbf{w} = (\rho Y_1, ..., \rho Y_{ns}, \rho \mathbf{u}, \rho E)^T \tag{1}$$

Numerical challenges [3]

- Multiscales in time and space $\Rightarrow$ *Splitting operators with adapted solver*
- Compressible effects
- Non callorically perfect gas

3. Tenaud, Roussel et Bentaleb, *Computers & Fluids* (2015).

Numerical tools/MR_CHORUS solver

Navier-Stokes equation

$$\mathbf{w}_t + \nabla \cdot (\mathbf{F}^E(\mathbf{w}) - \mathbf{F}^V(\mathbf{w}, \nabla\mathbf{w})) = \mathbf{S}(\mathbf{w}), \quad \text{with} \quad \mathbf{w} = (\rho Y_1, ..., \rho Y_{ns}, \rho\mathbf{u}, \rho E)^T \tag{1}$$

Numerical challenges [3]

- Multiscales in time and space $\Rightarrow$ *Splitting operators with adapted solver / Adaptive refinement*
- Compressible effects
- Non callorically perfect gas

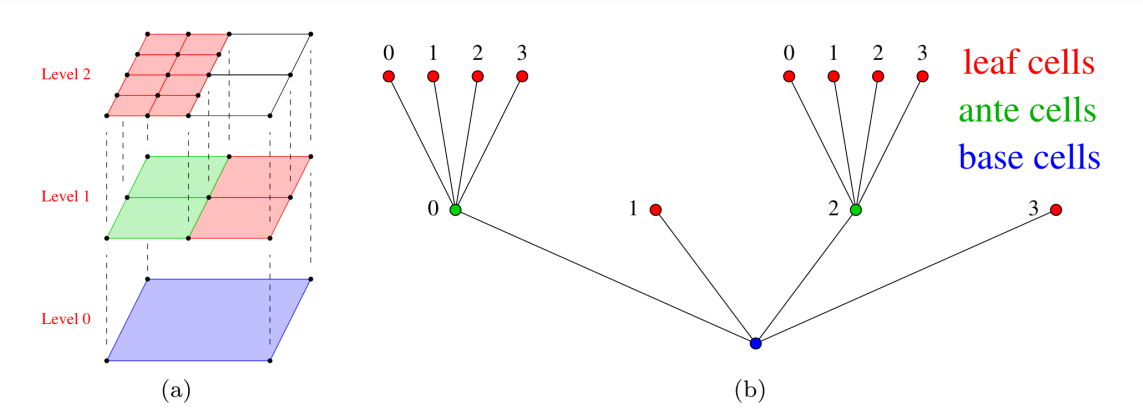

Figure 2 – Multiresolution approach with dynamic graded Tree

3. Tenaud, Roussel et Bentaleb, *Computers & Fluids* (2015).

Numerical tools/MR_CHORUS solver

Navier-Stokes equation

$$\mathbf{w}_t + \nabla \cdot (\mathbf{F}^E(\mathbf{w}) - \mathbf{F}^V(\mathbf{w}, \nabla\mathbf{w})) = \mathbf{S}(\mathbf{w}), \quad \text{with} \quad \mathbf{w} = (\rho Y_1, \ldots, \rho Y_{ns}, \rho\mathbf{u}, \rho E)^T \tag{1}$$

Numerical challenges [3]

- Multiscales in time and space $\Rightarrow$ *Splitting operators with adapted solver / Adaptive refinement*
- Compressible effects $\Rightarrow$ *Riemann approximate solver with flux limiter (OSMP scheme)*
- Non callorically perfect gas

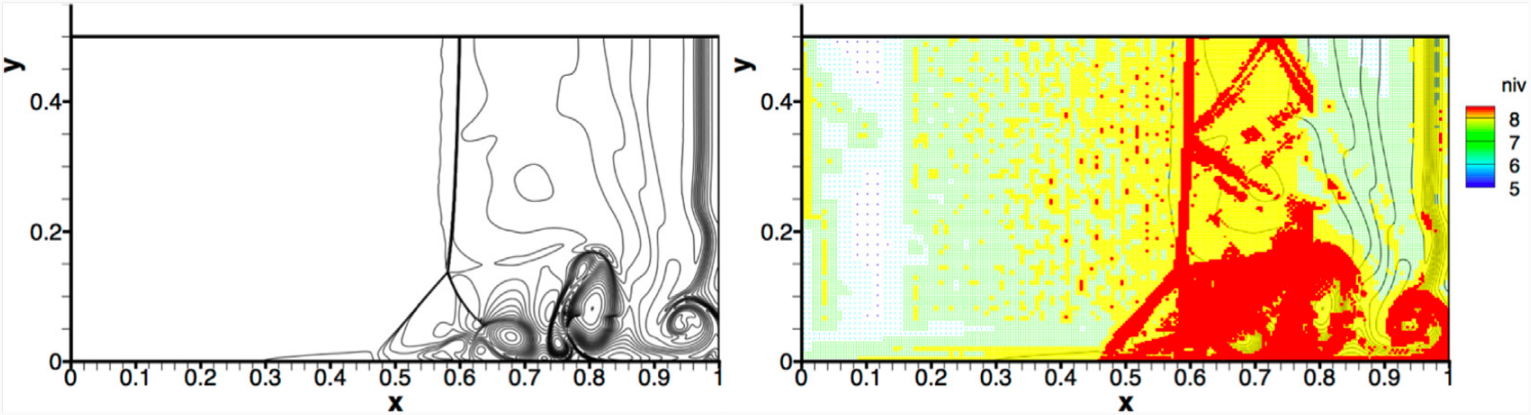

Figure 2 – Shock/boundary layer interaction. Isocontour of density and refined grid

3. Tenaud, Roussel et Bentaleb, *Computers & Fluids* (2015).

Numerical tools/MR_CHORUS solver

Navier-Stokes equation

$$\mathbf{w}_t + \nabla \cdot (\mathbf{F}^E(\mathbf{w}) - \mathbf{F}^V(\mathbf{w}, \nabla\mathbf{w})) = \mathbf{S}(\mathbf{w}), \quad \text{with} \quad \mathbf{w} = (\rho Y_1, ..., \rho Y_{ns}, \rho\mathbf{u}, \rho E)^T \tag{1}$$

Numerical challenges [3]

- Multiscales in time and space $\Rightarrow$ *Splitting operators with adapted solver / Adaptive refinement*
- Compressible effects $\Rightarrow$ *Riemann approximate solver with flux limiter (OSMP scheme)*
- Non callorically perfect gas $\Rightarrow$ *Extension of the Roe solver to realistic thermodynamic models*

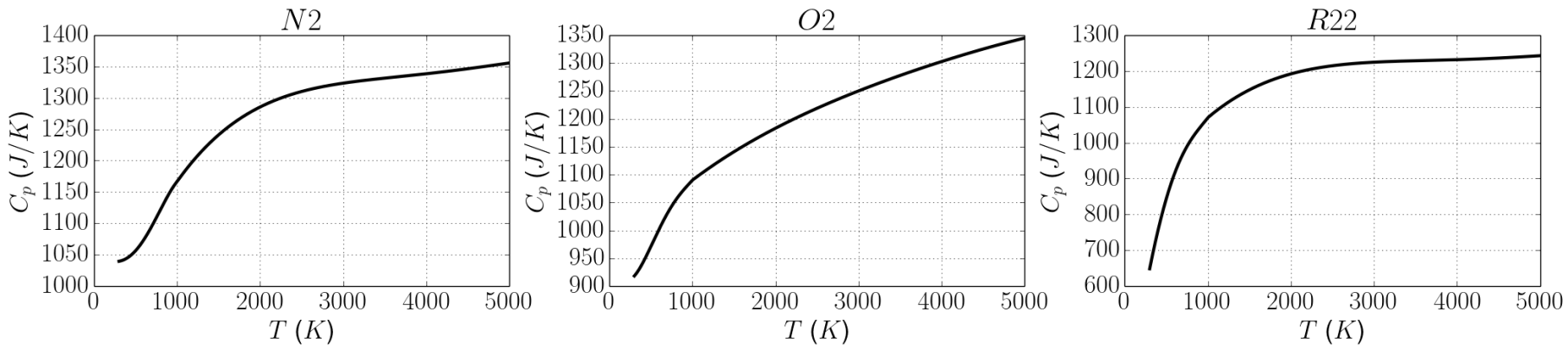

Figure 2 – Dependence of heat capacities on temperature with NASA polynomials

3. Tenaud, Roussel et Bentaleb, *Computers & Fluids* (2015).

OSMP scheme

Roe Approximate Riemann Solver

Roe Solver [4]

Roe's approach replace the Jacobian matrix evaluated at the intersection $\underline{\underline{\mathbf{A}}}(\mathbf{w}) = \partial \mathbf{F}^E(\mathbf{w})/\partial \mathbf{w}$ by a constant Jacobian matrix evaluated at the Roe average state $\overline{\mathbf{w}}$ combination of left $\mathbf{w}_L$ and right states $\mathbf{w}_R$

$$\underline{\underline{\mathbf{A}}}(\overline{\mathbf{w}}) = \underline{\underline{\mathbf{A}}}(\mathbf{w}_L, \mathbf{w}_R) \tag{2}$$

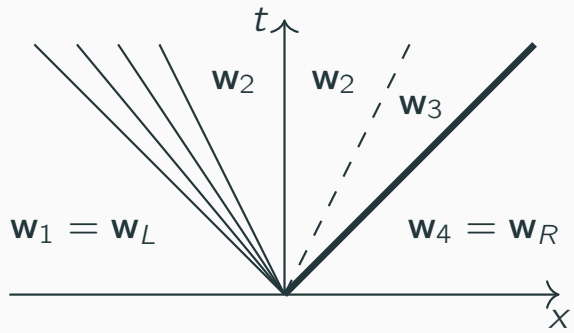

4. Roe, *Journal of Computational Physics* (1981).

Roe Approximate Riemann Solver

Roe Solver [4]

Roe's approach replace the Jacobian matrix evaluated at the intersection $\underline{\underline{\mathbf{A}}}(\mathbf{w}) = \partial \mathbf{F}^E(\mathbf{w})/\partial \mathbf{w}$ by a constant Jacobian matrix evaluated at the Roe average state $\overline{\mathbf{w}}$ combination of left $\mathbf{w}_L$ and right states $\mathbf{w}_R$

$$\underline{\underline{\mathbf{A}}}(\overline{\mathbf{w}}) = \underline{\underline{\mathbf{A}}}(\mathbf{w}_L, \mathbf{w}_R) \tag{2}$$

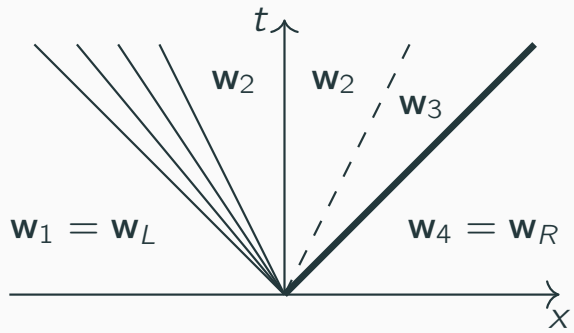

With non ideal gases

$$\underline{\underline{\mathbf{A}}}(\overline{\mathbf{w}}) = \underline{\underline{\mathbf{A}}}(\overline{\rho}, \overline{Y}_1, ..., \overline{Y}_{ns}, \overline{\mathbf{u}}, \overline{h}, \overline{\chi}_1, ...\overline{\chi}_{ns}, \overline{\kappa}) \tag{3}$$

with compressibility factors

$$\chi_i = \left(\frac{\partial p}{\partial \rho_i}\right)_{\tilde{\epsilon}, \rho_{k,k\neq i}} \quad \text{and} \quad \kappa = \left(\frac{\partial p}{\partial \tilde{\epsilon}}\right)_{\rho_k} \tag{4}$$

4. Roe, *Journal of Computational Physics* (1981).

Roe Approximate Riemann Solver

Roe Solver [4]

Roe's approach replace the Jacobian matrix evaluated at the intersection $\underline{\underline{\mathbf{A}}}(\mathbf{w}) = \partial \mathbf{F}^E(\mathbf{w})/\partial \mathbf{w}$ by a constant Jacobian matrix evaluated at the Roe average state $\overline{\mathbf{w}}$ combination of left $\mathbf{w}_L$ and right states $\mathbf{w}_R$

$$\underline{\underline{\mathbf{A}}}(\overline{\mathbf{w}}) = \underline{\underline{\mathbf{A}}}(\mathbf{w}_L, \mathbf{w}_R) \tag{2}$$

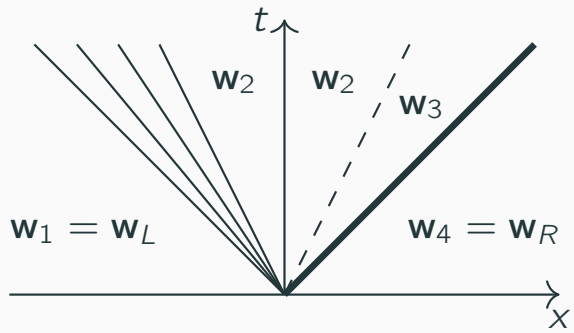

With non ideal gases

$$\underline{\underline{\mathbf{A}}}(\overline{\mathbf{w}}) = \underline{\underline{\mathbf{A}}}(\overline{\rho}, \overline{Y}_1, ..., \overline{Y}_{ns}, \overline{\mathbf{u}}, \overline{h}, \overline{\chi}_1, ...\overline{\chi}_{ns}, \overline{\kappa}) \tag{3}$$

with compressibility factors

$$\chi_i = \left(\frac{\partial p}{\partial \rho_i}\right)_{\tilde{\epsilon}, \rho_{k,k\neq i}} \quad \text{and} \quad \kappa = \left(\frac{\partial p}{\partial \tilde{\epsilon}}\right)_{\rho_k} \tag{4}$$

Flux expression

$$\mathbf{F}^{Roe}_{i+\frac{1}{2}} = \frac{1}{2}(\mathbf{F}_L + \mathbf{F}_R) - \frac{1}{2}\sum_{i=1}^{m} \delta\overline{\zeta}_i |\overline{\lambda}_i| \overline{\mathbf{r}}^{(i)} \tag{5}$$

with $\overline{\lambda_i}$, $\overline{\mathbf{r}}^{(i)}$ and $\overline{\zeta}_i$ eigenvalues, eigenvectors and Riemann invariants of $\underline{\underline{\mathbf{A}}}(\overline{\mathbf{w}})$

4. Roe, *Journal of Computational Physics* (1981).

Roe Average state

$$\underline{\underline{\mathbf{A}}}(\overline{\mathbf{w}}) = \underline{\underline{\mathbf{A}}}(\overline{\rho}, \overline{Y}_1, ..., \overline{Y}_{ns}, \overline{\mathbf{u}}, \overline{h}, \overline{\chi}_1, ...\overline{\chi}_{ns}, \overline{\kappa})$$

Rule for the construction of the Roe Average State

$$\boxed{\underline{\underline{\mathbf{A}}}(\overline{\mathbf{w}})(\mathbf{w}_L - \mathbf{w}_R) = \mathbf{F}(\mathbf{w}_L) - \mathbf{F}(\mathbf{w}_R)} \tag{6}$$

5. Vinokur et Montagné, *Journal of Computational Physics* (1990).

Roe Average state

$$\underline{\underline{\mathbf{A}}}(\overline{\mathbf{w}}) = \underline{\underline{\mathbf{A}}}(\overline{\rho}, \overline{Y}_1, ..., \overline{Y}_{ns}, \overline{\mathbf{u}}, \overline{h}, \overline{\chi}_1, ...\overline{\chi}_{ns}, \overline{\kappa})$$

Rule for the construction of the Roe Average State

$$\boxed{\underline{\underline{\mathbf{A}}}(\overline{\mathbf{w}})(\mathbf{w}_L - \mathbf{w}_R) = \mathbf{F}(\mathbf{w}_L) - \mathbf{F}(\mathbf{w}_R)} \tag{6}$$

Roe average operator for primitive/conservatives variables

$$\{\rho, Y_k, \mathbf{u}, h\} \quad \Rightarrow \quad \overline{(\cdot)} = \theta(\cdot)_L + (1-\theta)(\cdot)_R \qquad \text{with} \qquad \theta = \frac{\sqrt{\rho_L}}{\sqrt{\rho_L} + \sqrt{\rho_R}} \tag{7}$$

5. Vinokur et Montagné, *Journal of Computational Physics* (1990).

Roe Average state

$$\underline{\underline{\mathbf{A}}}(\overline{\mathbf{w}}) = \underline{\underline{\mathbf{A}}}(\overline{\rho}, \overline{Y}_1, ..., \overline{Y}_{ns}, \overline{\mathbf{u}}, \overline{h}, \overline{\chi}_1, ...\overline{\chi}_{ns}, \overline{\kappa})$$

Rule for the construction of the Roe Average State

$$\boxed{\underline{\underline{\mathbf{A}}}(\overline{\mathbf{w}})(\mathbf{w}_L - \mathbf{w}_R) = \mathbf{F}(\mathbf{w}_L) - \mathbf{F}(\mathbf{w}_R)} \tag{6}$$

Roe average operator for primitive/conservatives variables

$$\{\rho, Y_k, \mathbf{u}, h\} \quad \Rightarrow \quad \overline{(\cdot)} = \theta(\cdot)_L + (1-\theta)(\cdot)_R \qquad \text{with} \qquad \theta = \frac{\sqrt{\rho_L}}{\sqrt{\rho_L} + \sqrt{\rho_R}} \tag{7}$$

Treatment of the compressibility factors χ_i and κ

$$\left.\begin{array}{c} \underline{\underline{\mathbf{A}}}(\overline{\mathbf{w}})(\mathbf{w}_L - \mathbf{w}_R) = \mathbf{F}(\mathbf{w}_L) - \mathbf{F}(\mathbf{w}_R) \\ + \\ \boxed{\text{Roe average operator}} \end{array}\right\} \quad \Rightarrow \quad \Delta p = \sum_{i=0}^{ns} \overline{\chi}_i \Delta \rho_i + \overline{\kappa} \Delta \tilde{\epsilon} \tag{8}$$

5. Vinokur et Montagné, *Journal of Computational Physics* (1990).

Roe Average state

$$\underline{\underline{\mathbf{A}}}(\overline{\mathbf{w}}) = \underline{\underline{\mathbf{A}}}(\overline{\rho}, \overline{Y}_1, ..., \overline{Y}_{ns}, \overline{\mathbf{u}}, \overline{h}, \overline{\chi}_1, ...\overline{\chi}_{ns}, \overline{\kappa})$$

Rule for the construction of the Roe Average State

$$\boxed{\underline{\underline{\mathbf{A}}}(\overline{\mathbf{w}})(\mathbf{w}_L - \mathbf{w}_R) = \mathbf{F}(\mathbf{w}_L) - \mathbf{F}(\mathbf{w}_R)} \tag{6}$$

Roe average operator for primitive/conservatives variables

$$\{\rho, Y_k, \mathbf{u}, h\} \quad \Rightarrow \quad \overline{(\cdot)} = \theta(\cdot)_L + (1-\theta)(\cdot)_R \qquad \text{with} \qquad \theta = \frac{\sqrt{\rho_L}}{\sqrt{\rho_L} + \sqrt{\rho_R}} \tag{7}$$

Treatment of the compressibility factors χ_i and κ

$$\left.\begin{array}{c} \underline{\underline{\mathbf{A}}}(\overline{\mathbf{w}})(\mathbf{w}_L - \mathbf{w}_R) = \mathbf{F}(\mathbf{w}_L) - \mathbf{F}(\mathbf{w}_R) \\ + \\ \boxed{\text{Roe average operator}} \end{array}\right\} \quad \Rightarrow \quad \Delta p = \sum_{i=0}^{ns} \overline{\chi}_i \Delta \rho_i + \overline{\kappa} \Delta \tilde{\epsilon} \tag{8}$$

Approximation of the compressibility factors with method of Vinokur and Montagné [5] :

$$\hat{\kappa} = \int_0^1 \kappa[\rho(t), \tilde{\epsilon}(t)]dt \qquad \hat{\chi}_i = \int_0^1 \chi_i[\rho(t), \tilde{\epsilon}(t)]dt \tag{9}$$

5. Vinokur et Montagné, *Journal of Computational Physics* (1990).

Roe Average state

$$\underline{\underline{\mathbf{A}}}(\overline{\mathbf{w}}) = \underline{\underline{\mathbf{A}}}(\overline{\rho}, \overline{Y}_1, ..., \overline{Y}_{ns}, \overline{\mathbf{u}}, \overline{h}, \overline{\chi}_1, ...\overline{\chi}_{ns}, \overline{\kappa})$$

Rule for the construction of the Roe Average State

$$\boxed{\underline{\underline{\mathbf{A}}}(\overline{\mathbf{w}})(\mathbf{w}_L - \mathbf{w}_R) = \mathbf{F}(\mathbf{w}_L) - \mathbf{F}(\mathbf{w}_R)} \tag{6}$$

Roe average operator for primitive/conservatives variables

$$\{\rho, Y_k, \mathbf{u}, h\} \quad \Rightarrow \quad \overline{(\cdot)} = \theta(\cdot)_L + (1-\theta)(\cdot)_R \qquad \text{with} \qquad \theta = \frac{\sqrt{\rho_L}}{\sqrt{\rho_L} + \sqrt{\rho_R}} \tag{7}$$

Treatment of the compressibility factors χ_i and κ

$$\left.\begin{array}{c} \underline{\underline{\mathbf{A}}}(\overline{\mathbf{w}})(\mathbf{w}_L - \mathbf{w}_R) = \mathbf{F}(\mathbf{w}_L) - \mathbf{F}(\mathbf{w}_R) \\ + \\ \boxed{\text{Roe average operator}} \end{array}\right\} \quad \Rightarrow \quad \Delta p = \sum_{i=0}^{ns} \overline{\chi}_i \Delta \rho_i + \overline{\kappa} \Delta \tilde{\epsilon} \tag{8}$$

Approximation of the compressibility factors with method of Vinokur and Montagné [5] :

$$\hat{\kappa} = \int_0^1 \kappa[\rho(t), \tilde{\epsilon}(t)]dt \qquad \hat{\chi}_i = \int_0^1 \chi_i[\rho(t), \tilde{\epsilon}(t)]dt \tag{9}$$

Orthogonal projection on the $ns-1$ dimension hyperplane defined by (8)

$$\overline{\kappa} = \mathcal{P}(\hat{\kappa}) \qquad \overline{\chi}_i = \mathcal{P}(\hat{\chi}_i) \tag{10}$$

5. Vinokur et Montagné, *Journal of Computational Physics* (1990).

High order extension with OSMP scheme

One step monotonocity preserving (OSMP) scheme [6]

New system of advection equations

$$\frac{\partial \overline{\zeta}_i}{\partial t} + \overline{\lambda}_i \frac{\partial \overline{\zeta}_i}{\partial x} = 0 \quad \text{with} \quad \Lambda = (u, ..., u, u - \overline{c}_s, u + \overline{c}_s)^T \tag{11}$$

6. V.Daru et Tenaud, *Journal of Computational Physics* (2004).

High order extension with OSMP scheme

One step monotonocity preserving (OSMP) scheme [6]

New system of advection equations

$$\frac{\partial \overline{\zeta}_i}{\partial t} + \overline{\lambda}_i \frac{\partial \overline{\zeta}_i}{\partial x} = 0 \quad \text{with} \quad \Lambda = (u, ..., u, u - \overline{c}_s, u + \overline{c}_s)^T \tag{11}$$

Increase order in time and space with Lax-Wendroff procedure

$$\mathbf{F}^o_{j+1/2} = \mathbf{F}^{Roe}_{j+1/2} + \frac{1}{2} \sum_k (\Phi^o \mathbf{r})_{k,j+1/2} \tag{12}$$

Flux limiter : Monotonicity preserving scheme (TVD scheme with improvement near extrema)

$$\Phi^{o-MP} = \max(\Phi^{\min}, \min(\Phi^o, \Phi^{\max})) \tag{13}$$

6. V.Daru et Tenaud, *Journal of Computational Physics* (2004).

High order extension with OSMP scheme

One step monotonocity preserving (OSMP) scheme [6]

New system of advection equations

$$\frac{\partial \overline{\zeta}_i}{\partial t} + \overline{\lambda}_i \frac{\partial \overline{\zeta}_i}{\partial x} = 0 \quad \text{with} \quad \Lambda = (u, ..., u, u - \overline{c}_s, u + \overline{c}_s)^T \tag{11}$$

Increase order in time and space with Lax-Wendroff procedure

$$\mathbf{F}^o_{j+1/2} = \mathbf{F}^{Roe}_{j+1/2} + \frac{1}{2} \sum_k (\Phi^o \mathbf{r})_{k,j+1/2} \tag{12}$$

Flux limiter : Monotonicity preserving scheme (TVD scheme with improvement near extrema)

$$\Phi^{o-MP} = \max(\Phi^{\min}, \min(\Phi^o, \Phi^{\max})) \tag{13}$$

Riemann invariants recombination

Recomposition of the equations (11) with the same eigenvector u to improve flux limiter and keep relation between variation of mass fraction and variation of mass energy

$$\overline{\zeta}_1^{bis} = \sum_{i=1}^{ns} \overline{\zeta}_i \left(\overline{E}_c - \frac{\overline{\chi}_i}{\overline{\kappa}} \right) = \Delta(\rho E) + \overline{E}_c \Delta\rho - \overline{H} \frac{\Delta P}{\overline{c}^2} \tag{14}$$

6. V.Daru et Tenaud, *Journal of Computational Physics* (2004).

Numerical experiments

Realistic Thermodynamic model : Sod shock tube problem

Properties

- Sod shock tube with R22 gas, 640 cells and OSMP scheme of 7^{th} order
- Species data with thermodynamic NASA polynomials

	$0 \leq x \leq 25$	$25 < x \leq 50$
P (bar)	1	0.1
$\rho(kg/m^3)$	1	0.125
N_2 (%)	75.55	23.16
R_{22} (%)	23.16	75.55
O_2 (%)	1.29	1.29
γ	1.38	1.32

Table 1 – initial conditions

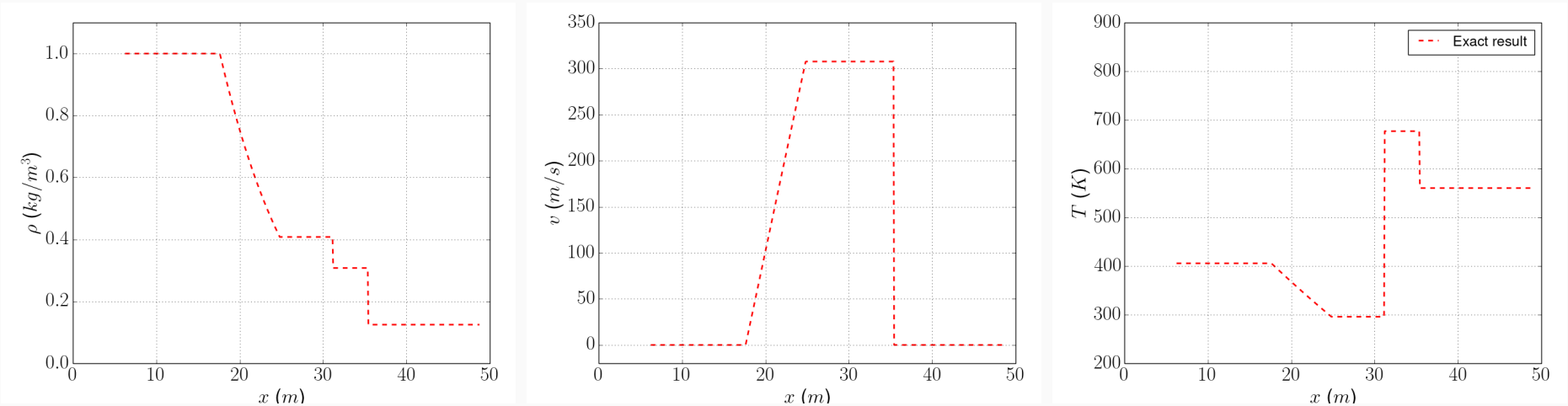

Figure 3 – Density, velocity and temperature profiles at t = 20ms

Realistic Thermodynamic model : Sod shock tube problem

Properties

- Sod shock tube with R22 gas, 640 cells and OSMP scheme of 7^{th} order
- Species data with thermodynamic NASA polynomials

	$0 \leq x \leq 25$	$25 < x \leq 50$
P (bar)	1	0.1
$\rho(kg/m^3)$	1	0.125
N_2 (%)	75.55	23.16
R_{22} (%)	23.16	75.55
O_2 (%)	1.29	1.29
γ	1.38	1.32

Table 1 – initial conditions

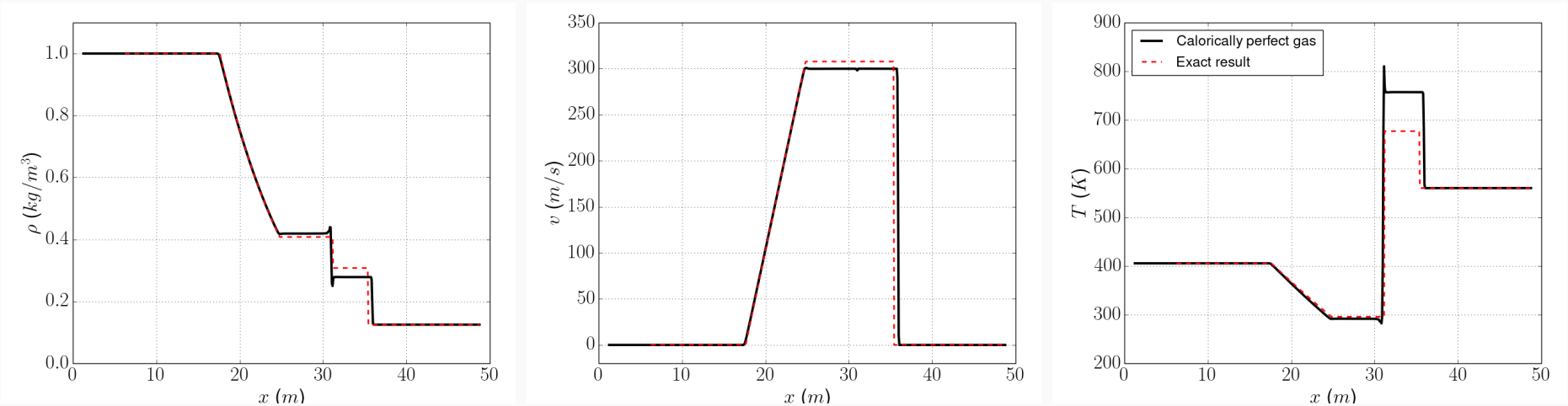

Figure 3 – Density, velocity and temperature profiles at t = 20ms

Realistic Thermodynamic model : Sod shock tube problem

Properties

- Sod shock tube with R22 gas, 640 cells and OSMP scheme of 7^{th} order
- Species data with thermodynamic NASA polynomials

	$0 \leq x \leq 25$	$25 < x \leq 50$
P (bar)	1	0.1
$\rho(kg/m^3)$	1	0.125
N_2 (%)	75.55	23.16
R_{22} (%)	23.16	75.55
O_2 (%)	1.29	1.29
γ	1.38	1.32

Table 1 – initial conditions

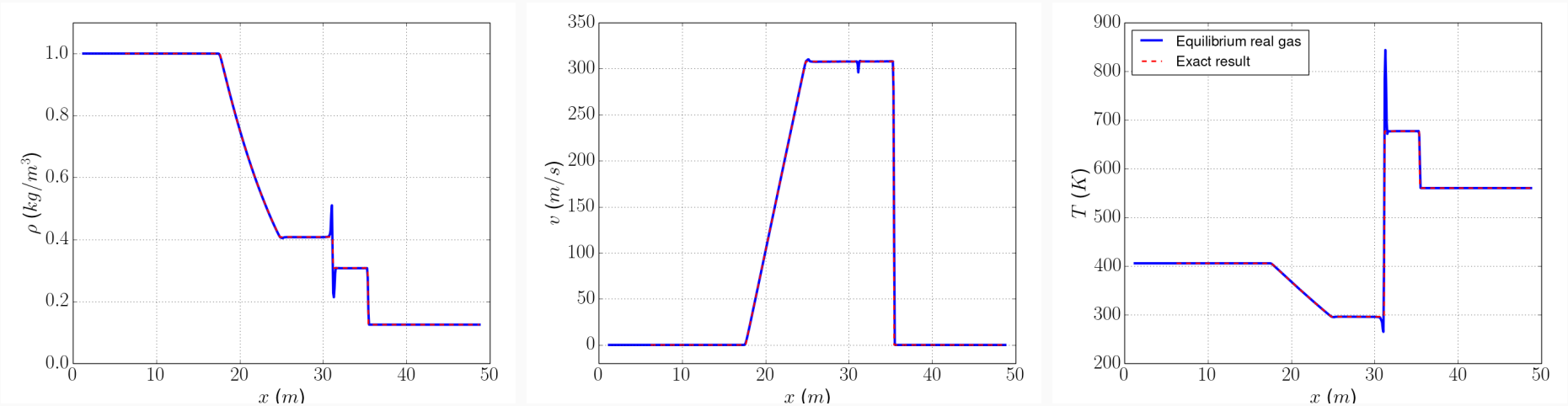

Figure 3 – Density, velocity and temperature profiles at t = 20ms

Realistic Thermodynamic model : Sod shock tube problem

Properties

- Sod shock tube with R22 gas, 640 cells and OSMP scheme of 7^{th} order
- Species data with thermodynamic NASA polynomials
- OSMP adapted with combination of Riemann invariants (14)

	$0 \leq x \leq 25$	$25 < x \leq 50$
P (bar)	1	0.1
$\rho(kg/m^3)$	1	0.125
N_2 (%)	75.55	23.16
R_{22} (%)	23.16	75.55
O_2 (%)	1.29	1.29
γ	1.38	1.32

Table 1 – initial conditions

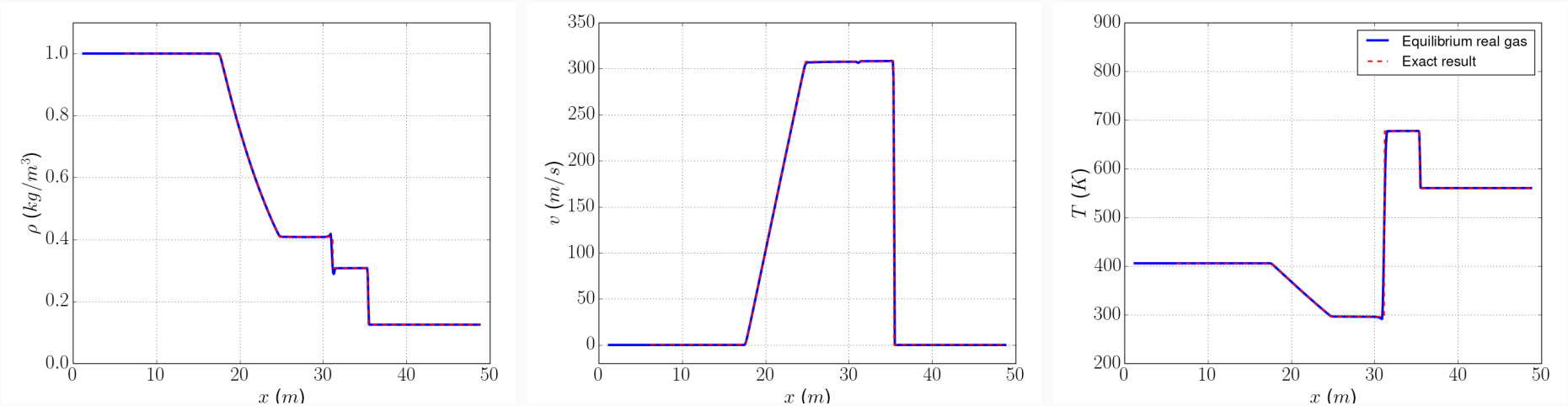

Figure 3 – Density, velocity and temperature profiles at t = 20ms

Hydrodynamic instability : shock/bubble interaction

Parameters

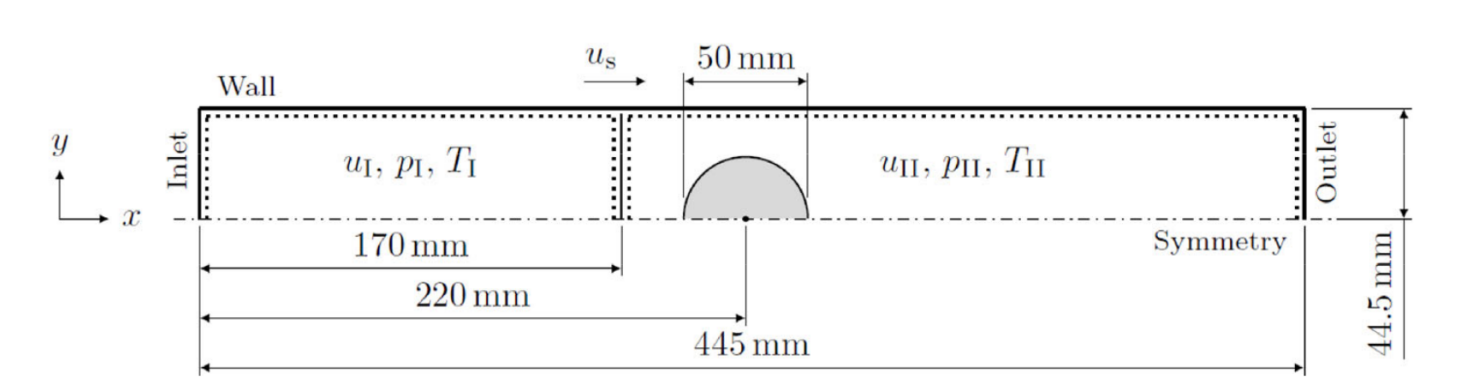

$p_{II} = 1Bar$,
$T_{II} = 351.82K$,
$M_s = 1.22$

OSMP 7^{th} order

Results

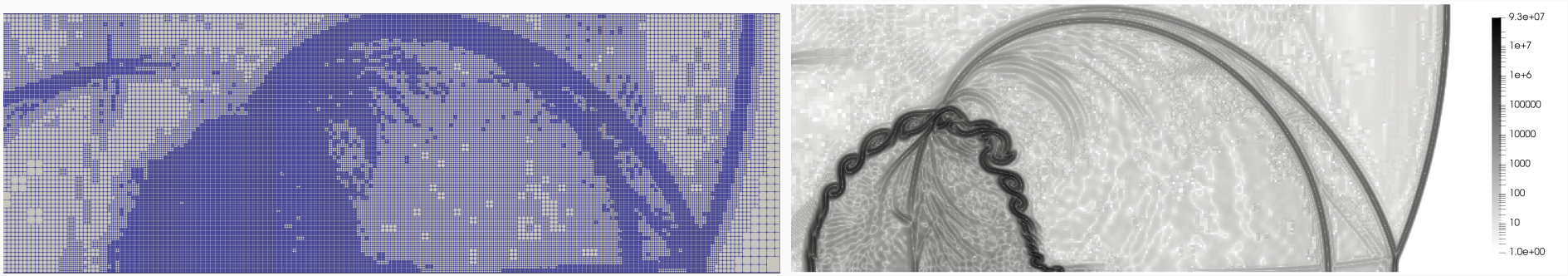

Figure 4 – Mesh and density gradient at $\tau = ta_{II,R22}/d_0 = 1.15$ for 256 cells in initial bubble diameter

Capture of Richtmyer–Meshkov instability with high order simulation

Reactive mixture : Detonation front

1D ZND structure

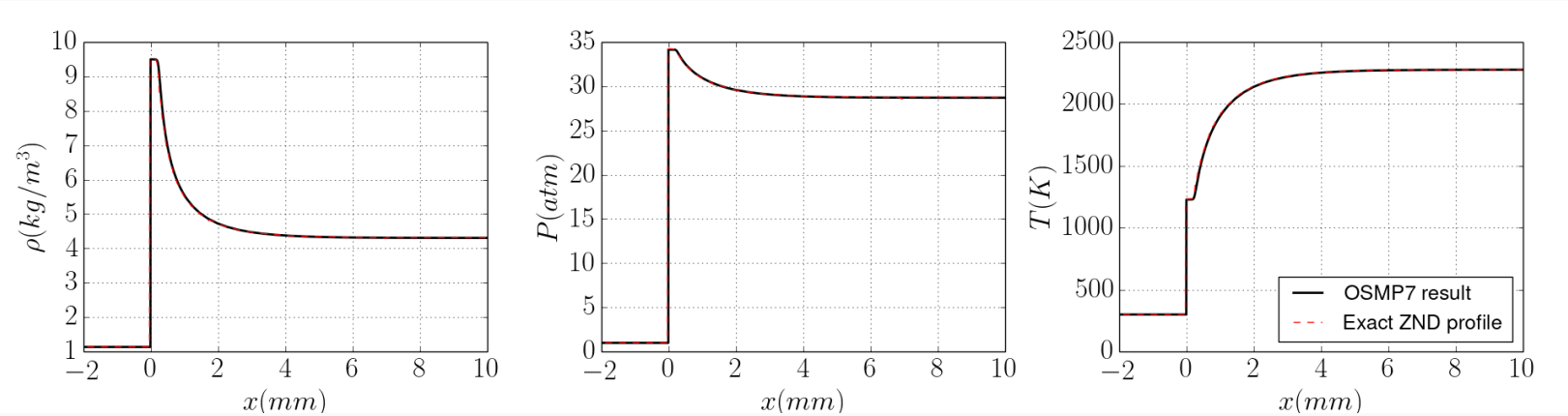

Respect stability criterion (heat release, induction length, overdriven velocity...) [7]

Unstable case

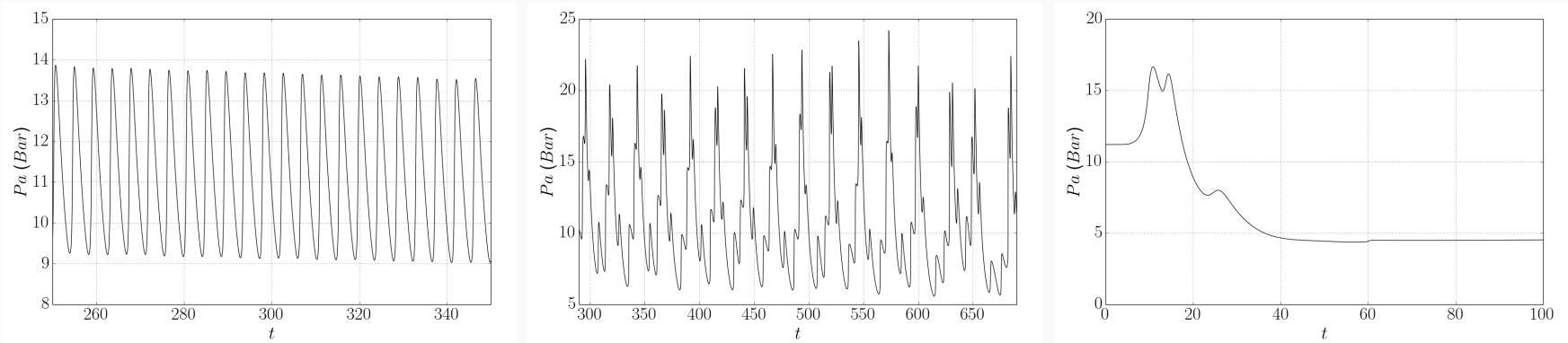

Figure 5 – Oscillation of post-shock pressure for increasing induction length until quenching

7. Ng et al., *Combustion Theory and Modelling* (2005).

Reactive mixture : Acceleration of flame

Detonation initiation by reflected shock

- Two-steps chemistry
- NASA poynomials

Reactive mixture : Acceleration of flame

Detonation initiation by reflected shock

- Two-steps chemistry
- NASA poynomials

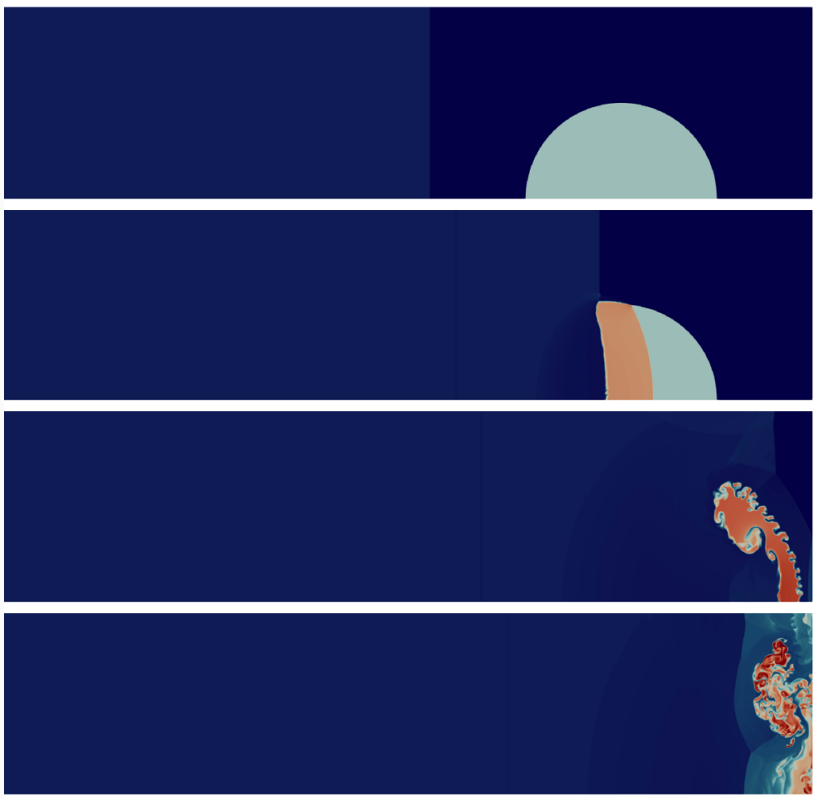

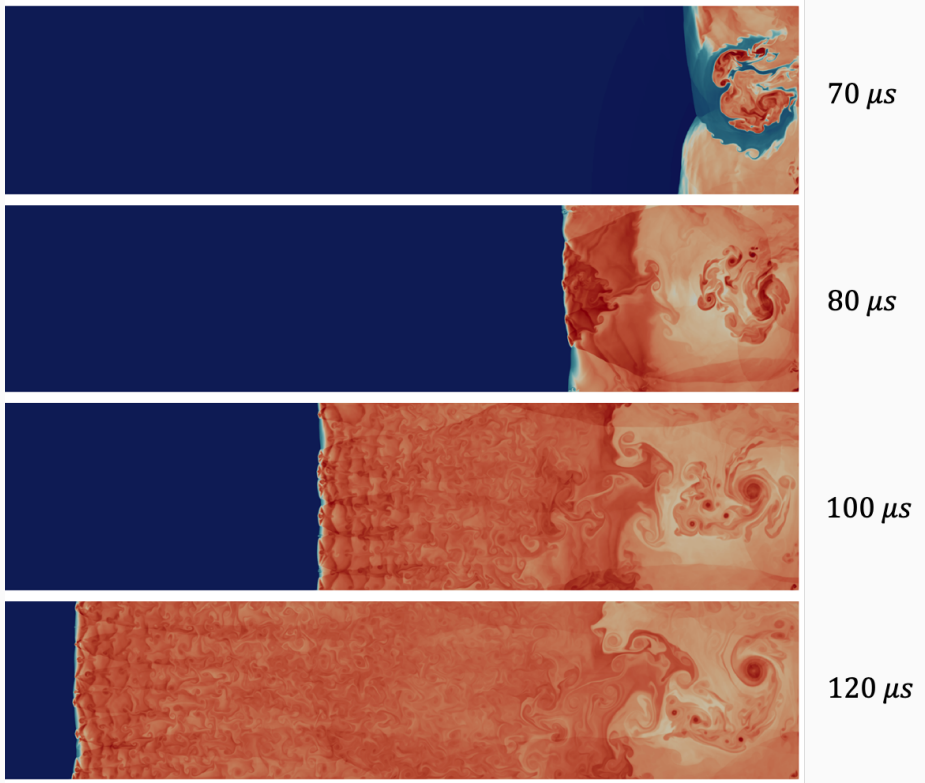

Reactive mixture : 2D Detonation

Detonation structure

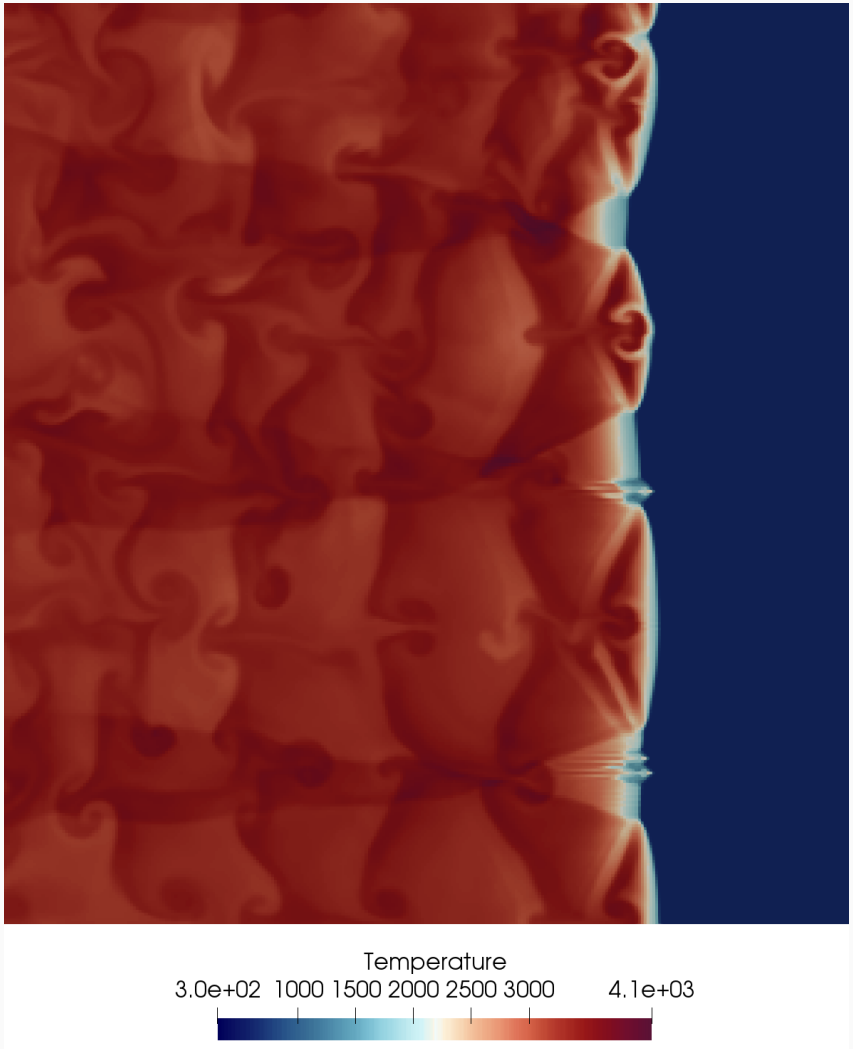

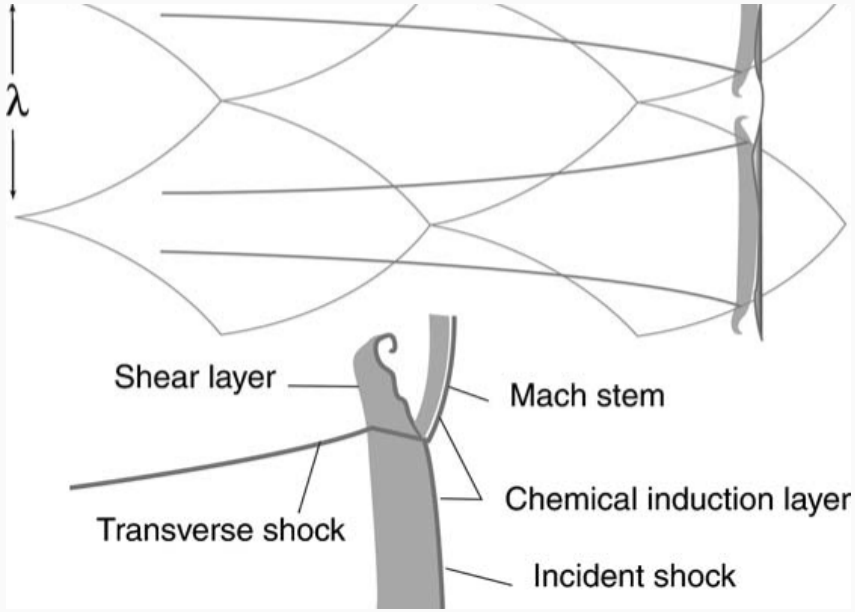

2D Detonation front

- Detonation cell
- Shear layer
- Chemical induction layer

Reactive mixture : 2D Detonation

Detonation structure

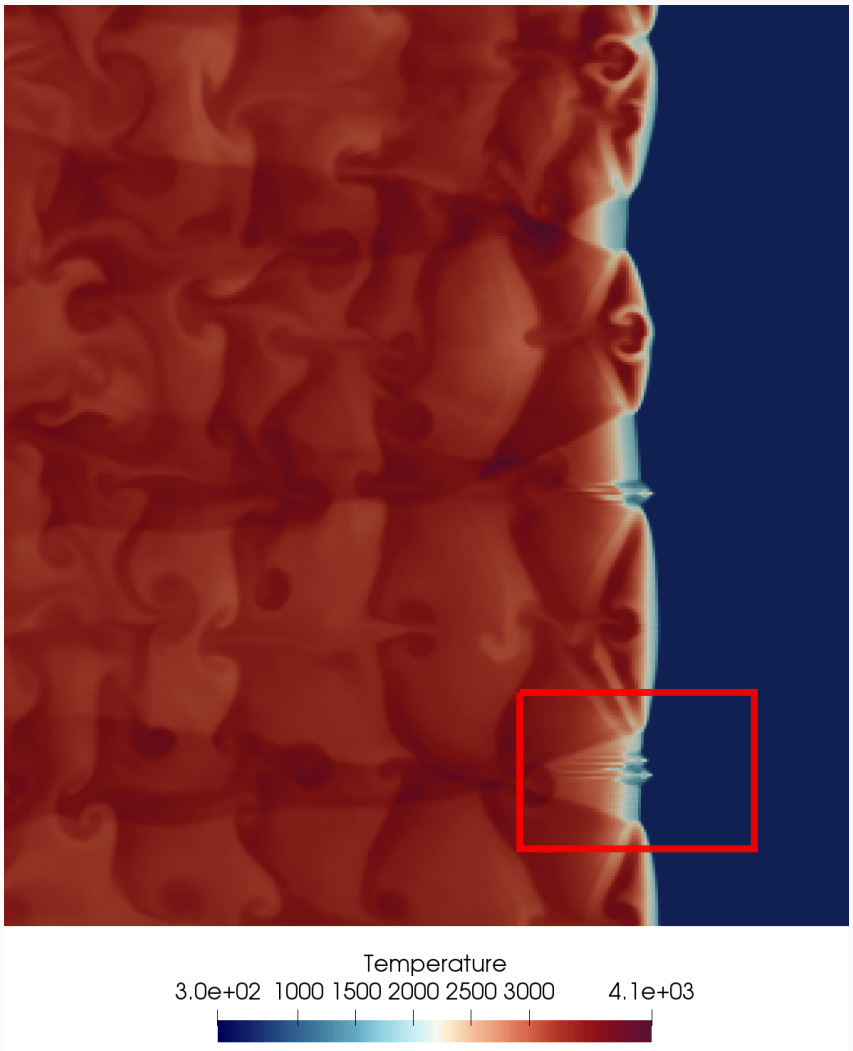

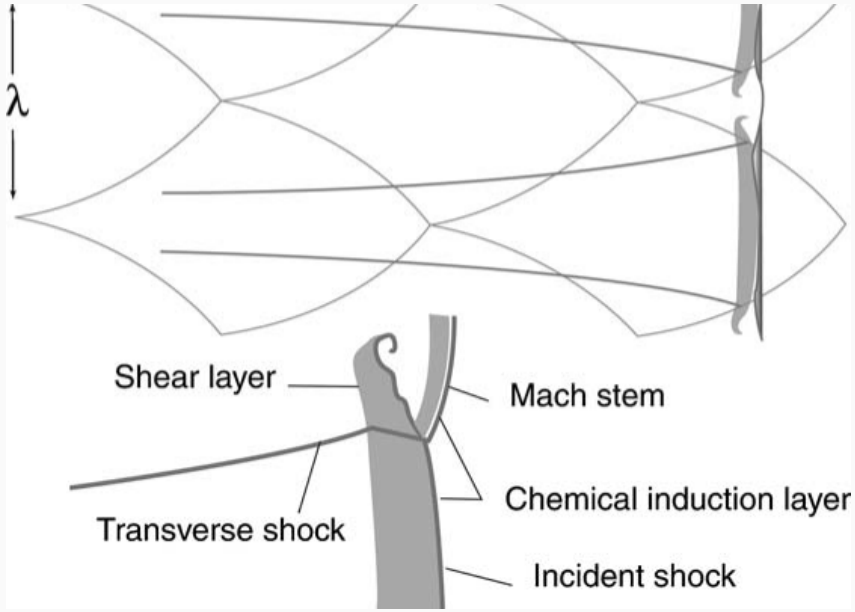

Carbuncle instability

- Insufficient cross-flow dissipation
- Specific to Complete Riemann solver
- Amplified phenomena with heat release

Cure the carbuncle instabilities

Rotated solver [8]

Rotational invariant property of Euler equation

$$(\hat{\mathbf{w}}_k)_t + (\mathbf{f}^E(\hat{\mathbf{w}}_k))_{\hat{x}} = 0 \tag{15}$$

with $\hat{\mathbf{w}}_k = \mathbf{T}_k \mathbf{w}_k$ and $\mathbf{T}_k$ rotation matrix

$$\mathbf{F}^{Roe}_{i+\frac{1}{2}} = \frac{1}{2}(\mathbf{F}_L + \mathbf{F}_R) - \frac{1}{2}\left[\sum_{m=1}^{2} |\alpha^m_{i+1/2}| \sum_{i=1}^{N} \delta\bar{\zeta}_i |\bar{\lambda}_i| \bar{\mathbf{r}}^{(i)}\right] \tag{16}$$

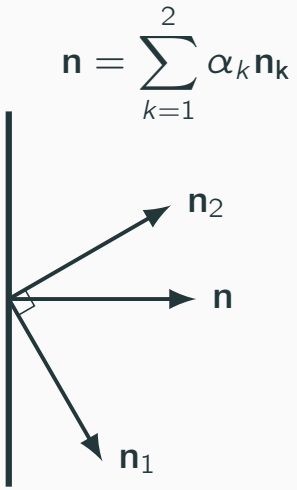

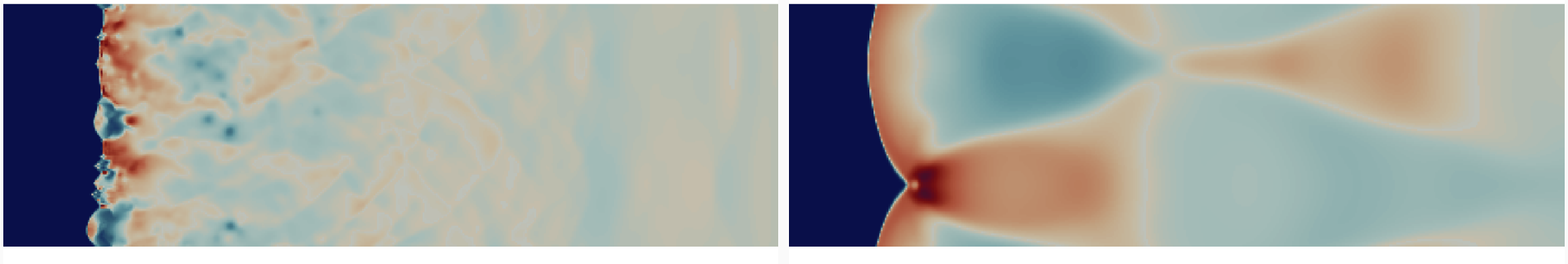

Figure 6 – Application of rotated solver

8. Ren, *Computers & Fluids* (2003).

Cure the carbuncle instabilities

Rotated solver [8]

Rotational invariant property of Euler equation

$$(\hat{\mathbf{w}}_k)_t + (\mathbf{f}^E(\hat{\mathbf{w}}_k))_{\hat{x}} = 0 \tag{15}$$

with $\hat{\mathbf{w}}_k = \mathbf{T}_k \mathbf{w}_k$ and $\mathbf{T}_k$ rotation matrix

$$\mathbf{F}^{Roe}_{i+\frac{1}{2}} = \frac{1}{2}(\mathbf{F}_L + \mathbf{F}_R) - \frac{1}{2}\left[\sum_{m=1}^{2} |\alpha^m_{i+1/2}| \sum_{i=1}^{N} \delta\bar{\zeta}_i |\bar{\lambda}_i| \bar{\mathbf{r}}^{(i)}\right] \tag{16}$$

$$\mathbf{n} = \sum_{k=1}^{2} \alpha_k \mathbf{n_k}$$

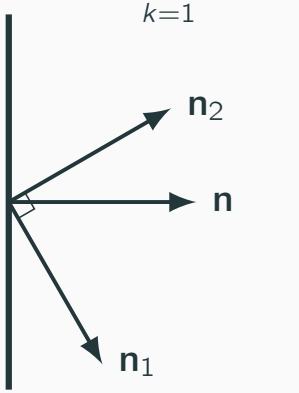

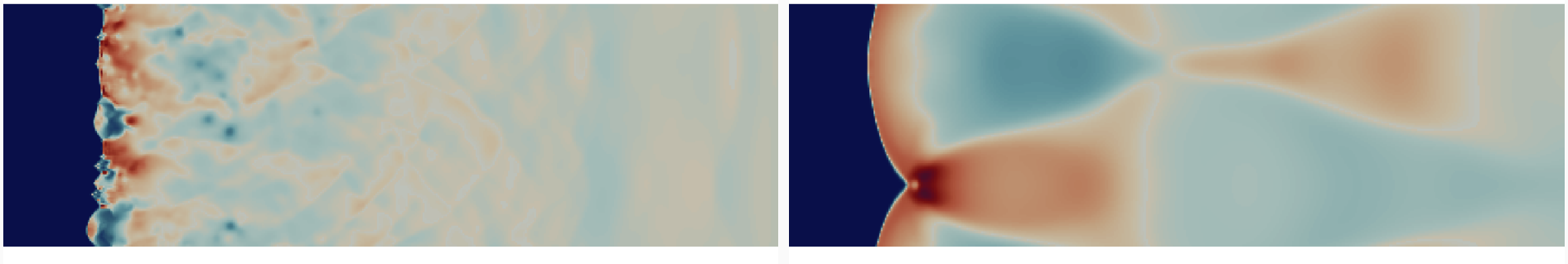

Figure 6 – Application of rotated solver

Not a high-order recomposition for now (diffusive solution)

8. Ren, *Computers & Fluids* (2003).

Conclusion

Conclusion

Objective : complete case study of hydrogen flame acceleration in 2D and 3D with geometrical configuration

High order compressible solver

- Extension of the approximate Riemann solver of Roe for multicomponent real gas flow
- OSMP scheme : new combination of Riemann invariants to capture correctly the contact wave

Validation tests

- Realistic Thermodynamic model for multispecies
- Capture hydrodynamic instabilities
- Flame acceleration/Detonation case without too strong shocks
- Carbuncle correction (only with low-order for now)

Conclusion

Objective : complete case study of hydrogen flame acceleration in 2D and 3D with geometrical configuration

High order compressible solver

- Extension of the approximate Riemann solver of Roe for multicomponent real gas flow
- OSMP scheme : new combination of Riemann invariants to capture correctly the contact wave

Validation tests

- Realistic Thermodynamic model for multispecies
- Capture hydrodynamic instabilities
- Flame acceleration/Detonation case without too strong shocks
- Carbuncle correction (only with low-order for now)
- 3D simulation
- Immersed boundary methods

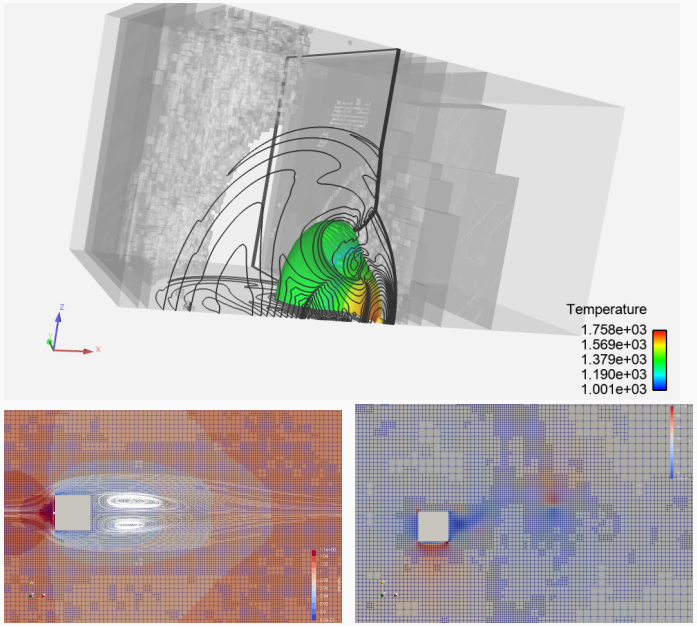

Thank you for your attention

Références

L. R. Boeck et al. “Detonation propagation in hydrogen–air mixtures with transverse concentration gradients”. In : *Shock Waves* 26 (2016), p. 181-192.

H. D. Ng et al. “Numerical investigation of the instability for one-dimensional Chapman–Jouguet detonations with chain-branching kinetics”. In : *Combustion Theory and Modelling* 9.3 (2005), p. 385-401.

Yu-Xin Ren. “A robust shock-capturing scheme based on rotated Riemann solvers”. In : *Computers & Fluids* 32.10 (2003), p. 1379 -1403.

P.L Roe. “Approximate Riemann solvers, parameter vectors, and difference schemes”. In : *Journal of Computational Physics* 43.2 (1981), p. 357 -372.

R. Scarpa et al. “Influence of initial pressure on hydrogen/air flame acceleration during severe accident in NPP”. In : *International Journal of Hydrogen Energy* 44.17 (2019). Special issue on The 7th International Conference on Hydrogen Safety (ICHS 2017), 11-13 September 2017, Hamburg, Germany, p. 9009 -9017.

Bibliography ii

Christian Tenaud, Olivier Roussel et Linda Bentaleb. “Unsteady compressible flow computations using an adaptive multiresolution technique coupled with a high-order one-step shock-capturing scheme”. In : *Computers & Fluids* 120 (2015), p. 111 -125.

V.Daru et C. Tenaud. “High order one-step monotonicity-preserving schemes for unsteady compressible flow calculations”. In : *Journal of Computational Physics* 193 (2004), p. 563-594.

Marcel Vinokur et Jean-Louis Montagné. “Generalized flux-vector splitting and Roe average for an equilibrium real gas”. In : *Journal of Computational Physics* 89.2 (1990), p. 276 -300.